

Laser Welding of T-Joints Made of Thin Austenitic Sheets

Abstract: The article presents test results concerning the CO₂ and Yb:YAG laser welding of thin-walled T-joints made of steel X5CrNi18-10 (steel 304), X6CrNi18-10 (steel 304H) and X15CrNiSi25-21 (steel 310) selected as stainless steels potentially useful in the production of ribbed pipes (finned tubes) intended for operation in boilers of supercritical parameters. Welding tests were performed using two different laser sources, i.e. a CO₂ gas laser and a Yb:YAG solid state laser. The tests involved the determination of the appropriate angle of laser beam insertion into the interface of sheets, enabling the obtainment of properly shaped welds. Non-destructive tests classified the joints as representing quality level B in accordance with standard 13919-1. Selected joints were tested for the distribution of alloying constituents in the joint area. It was ascertained that laser welding made it possible to maintain the uniform distribution of alloying constituents without their significant depletion in the weld area. The tests were financed using the funds of project PBS1/A5/13/2012.

Keywords: laser beam welding, T-joints, austenitic steel, CO₂ laser, Yb:YAG laser

DOI: [10.17729/ebis.2016.5/21](https://doi.org/10.17729/ebis.2016.5/21)

Introduction

The necessity of reducing the emission of pollutants defined in EU directives, e.g. 2001/77/EC, 2001/80/WE and 1997/97/23/WE requires changes in the design and construction of new flue gas desulphurisation units and the revamping of existing power units or the construction of new units having supercritical parameters. As units having supercritical parameters are operated at higher temperature and under higher pressure than those having subcritical parameters, they require to be made of materials characterised by higher creep and heat resistance. The notion of “supercritical parameters” refers mainly to power units intended for operation

at a steam temperature of 565÷620°C and under a pressure of 30 MPa whereas the notion of ultrasupercritical parameters refers to a steam temperature of 650÷720°C, a pressure of 35 MPa and a net efficiency of 45-50% [1-3].

Structural key elements of boilers used in power engineering are tubular elements of heat exchangers, including fin tubes with continuous or incised fins. Depending on the parameters of working media and flue gas, such elements can function as heaters, fuel economisers or superheaters. Fin tubes are used in order to multiply the area of heat exchange with the environment (approximately 30 times in comparison with smooth pipes). As a result, boilers utilising fin

dr inż. Sebastian Stano (PhD (DSc) Eng.); mgr inż. Jerzy Dworak (MSc Eng.), mgr inż. Michał Urbańczyk (MSc Eng.) – Instytut Spawalnictwa, Welding Technologies Department; dr hab. inż. Janusz Adamiec (PhD (DSc) hab. Eng.), Professor at Silesian University of Technology, Katowice, Poland

tubes can be fully optimised in terms of boiler heated areas and, consequently, in terms of boiler dimensions and weight. The use of fin tubes in industrial (power generation) boilers significantly increases their efficiency [5].

Welded fin tubes are usually made of weldable unalloyed steels (e.g. P235) and low alloy steels (e.g. C-Mo and C-CrMo steel grades 15Mo3, 13CrMo4.4 and 10CrMo4.10 according to DIN 17175). When designing units characterised by supercritical parameters, it was revealed that, because of the decrease in creep and oxidation resistance, the use of classical and martensitic steels in the power industry faces its limit at an operating temperature of 650°C. Designing elements enabling the obtainment of higher steam output parameters (up to 720°C and 35 MPa) required the use of austenitic steels (e.g. Super304 H) and/or nickel alloys (e.g. Inconel 617) [4].

Industries use many various technologies when making fin tubes, e.g. technologies enabling the production of divided joints (strip wound on a smooth tube) or welded joints maintaining metallic continuity between tubes and fins, characterised by better thermal efficiency. One of the most advanced welding technologies used when making tube-fin joints (T-joints with butt welds) is laser welding. The use of a concentrated heat source enables the formation of precise welds at very high welding rates, whereas appropriately adjusted process parameters ensure the satisfaction of acceptance criteria concerning pressure equipment [5].

The article contains certain results of the task entitled *Development of Technological Guidance on the Laser Welding of Austenitic Steels and Nickel Alloys* performed at Instytut Spawalnictwa within the project *Technology of the Laser Welding of Fin Tubes Made of Austenitic Steels and Nickel Alloys Intended for Operation in Boilers of Supercritical and Ultrasupercritical Parameters* financed by the National Centre for Research and Development (PBS1/A5/13/2012).

Tests

The purpose of the tests was to determine the possibility of using the CO₂ gas laser and the Yb:YAG solid-state laser when making T-joints of selected austenitic steels imitating the tube-fin joint used in fin tubes. The laser welding tests were performed in the Welding Technologies Laboratory of the Welding Technologies Department at Instytut Spawalnictwa. The laser welding technological tests were performed on two different stations equipped with two different types of laser resonators.

TRUMPF LaserCell 1005

The Lasercell TLC 1005 laser welding machine manufactured by Trumpf (Fig. 1) is equipped with a TLF type CO₂ gas laser having a power of 3.8 [kW] and emitting a radiation beam having a wavelength of 10.6 μm. The machine constitutes a laser processing centre used for the cutting and welding of flat (2D) and spatial (3D) elements. The working motion of the tool incorporates movements of 5 axes (x-axis and y-axis and two axes of rotation, i.e. B – ±120° and C – n × 360°). The laser welding tests involved the use of a welding head provided with a focusing mirror having focal length $f = 270$ mm. The head makes it possible to obtain a laser beam focus having a diameter of approximately 550 μm. The distribution of power density measured using a UFF100 laser beam analyser is presented in Figure 2.

Laser Processing Robot Station Equipped with the Solid-State Laser

Presently, robot stations provided with disc lasers belong to the most advanced and technically complicated welding systems used in various industries. The principal elements of the station are the following (Fig. 3):

- KUKA-KR 30/2 HA industrial robot (nominal lifting capacity: 30 kg; workspace: approximately 28.7 m³, positioning repeatability: ±0,1 mm),
- Laser TruDisk 12002 – Yb:YAG type laser

having a maximum power of 12 kW (laser beam quality identified using parameter $BPP \leq 8 \text{ mm} \times \text{mrad}$),

- set of optical fibres connecting the resonator with the welding head, including an optical fibre having a diameter of $300 \mu\text{m}$ (used in the tests),
- set of technological heads, including the CFO welding head used in the tests ($f_{kol} = 200 \text{ mm}$, $f_{og} = 300 \text{ mm}$, $d_{og} = 0.45 \text{ mm}$).

The distribution of power density measured using the UFF100 laser beam analyser is presented in Figure 4.

Test T-joints were made after placing and fixing flat bars using special fixtures ensuring the stable positioning and individual joint components. After laser cutting, the flat bars were degreased using acetone. Tack welds were not used.

An integral part of the fixtures was a nozzle enabling the flow of shielding gas used for the protection of weld roots. The nozzle was a tube having an internal diameter of 6 mm. The external surface of the nozzle was perforated (along its entire length) with openings having a diameter of 1 mm. The diameter of nozzle openings and their arrangement provided the laminar flow of shielding gas protecting the weld root. When the CO_2 gas laser was used, the weld face was protected by an additional side shielding gas nozzle having an internal diameter of 6 mm. The above named nozzle was used instead of a coaxial nozzle as the former provided the better protection of the weld face. Laser welding performed using the Yb:YAG solid-state laser involved the use of a multi-tube shielding gas nozzle. The shielding gas used in the tests was argon.

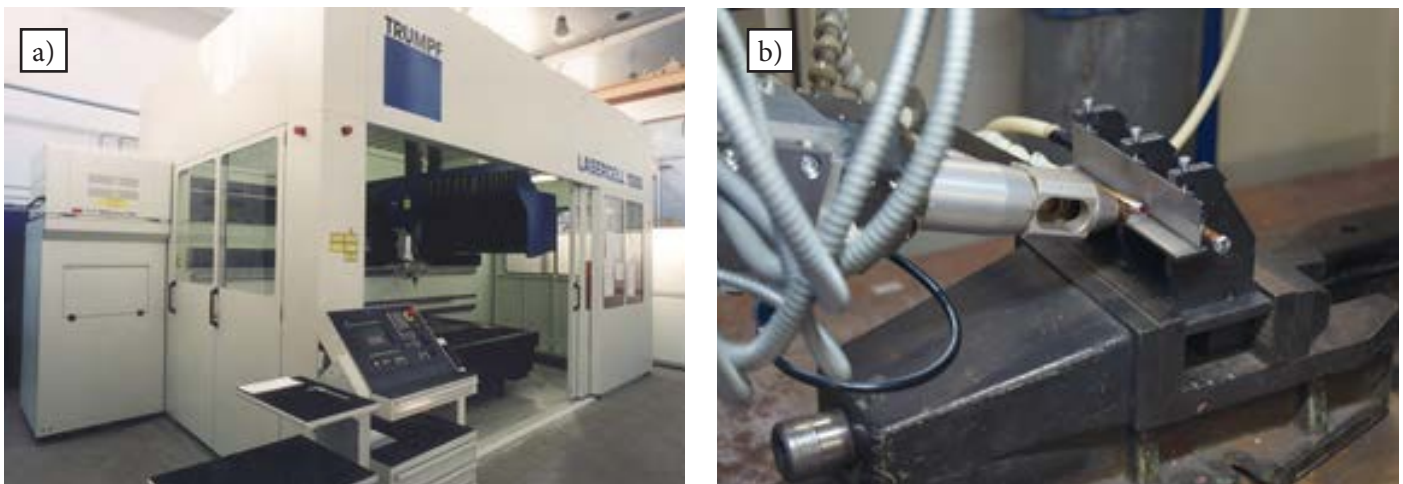


Fig. 1. Lasercell 1005 – the 3D laser processing centre equipped with the CO_2 laser having a power of 3.8 kW installed at Instytut Spawalnictwa: a – main view , b – welding head and fixtures for the laser welding of T-joints

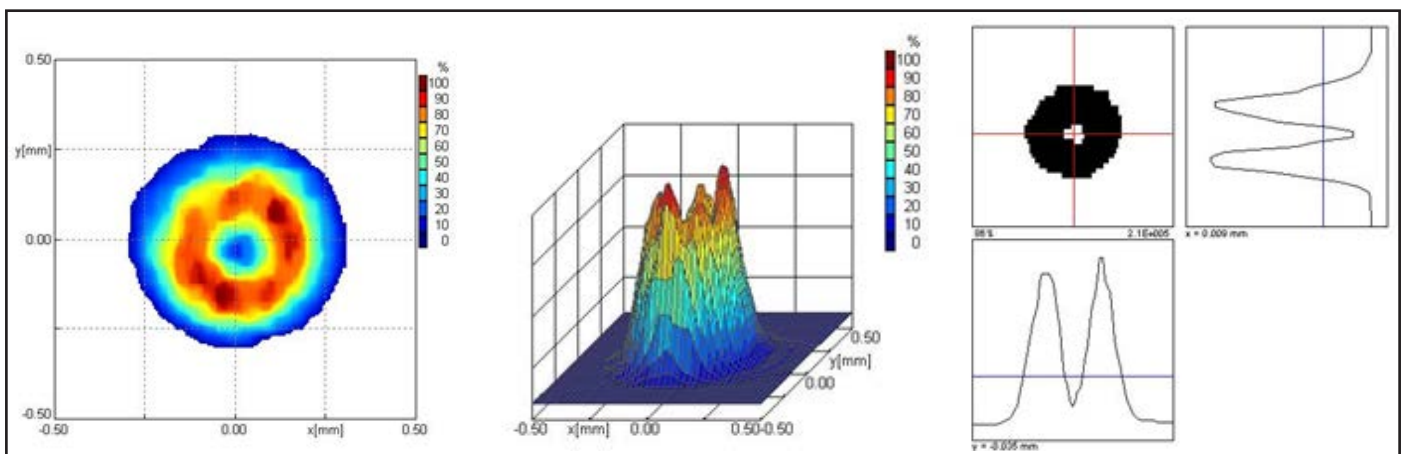


Fig. 2. Power density distribution of the CO_2 laser beam in the laser beam focus in the welding head used during the tests and having focal length $f = 270 \text{ mm}$

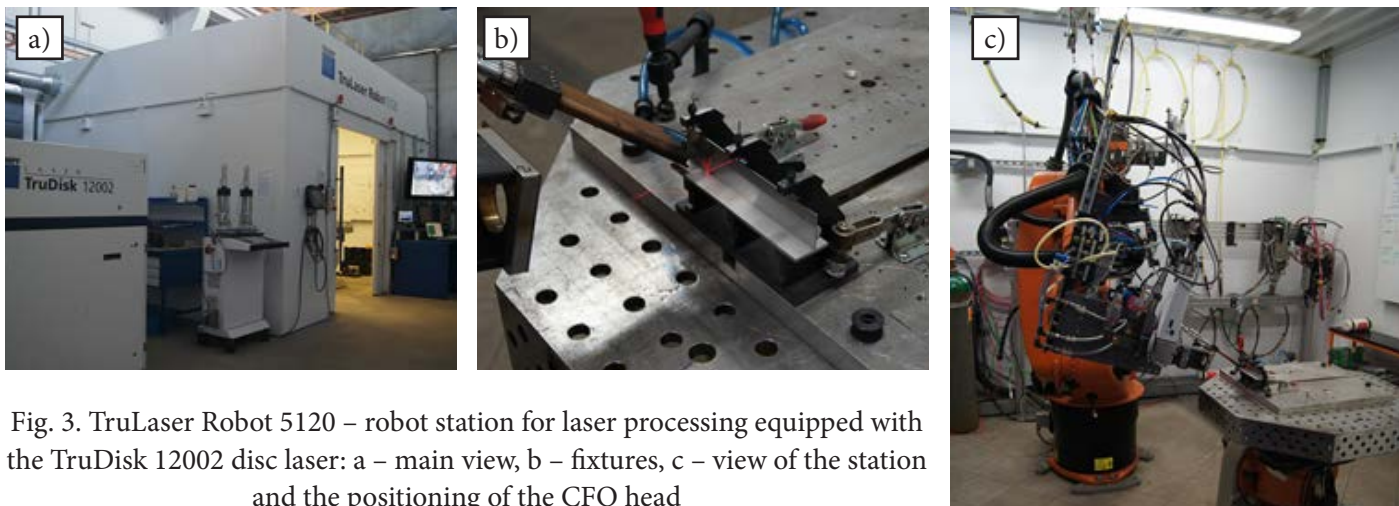


Fig. 3. TruLaser Robot 5120 – robot station for laser processing equipped with the TruDisk 12002 disc laser: a – main view, b – fixtures, c – view of the station and the positioning of the CFO head

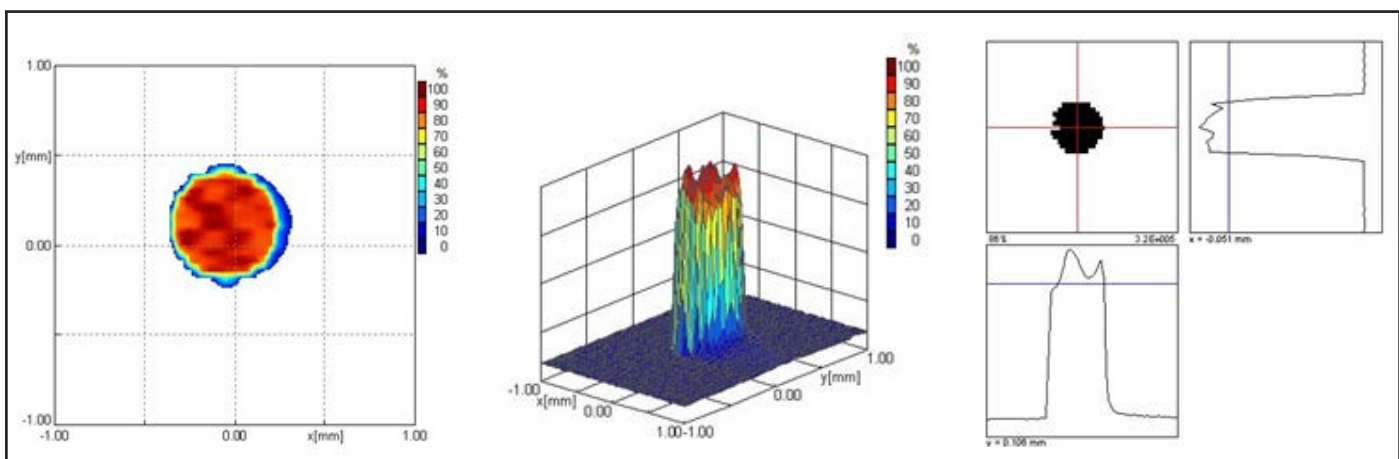


Fig. 4. Distribution of laser beam power density of the Yb:YAG TruDisk 12002 laser used in the tests in the laser beam focus for the CFO welding head

The macroscopic tests of the welded joints were performed using an SMZ 168 stereoscopic microscope manufactured by Motic. The chemical composition tests of base materials were performed using a Q4 TASMÁN 170 spark emission spectrometer made by Bruker. The tests of the welds in terms of the EDS method-based chemical composition in micro-areas were performed using a Zeiss Evo MA10 scanning electron microscope provided with an EDS Bruker XFlash® 5010 spectrometer. The results obtained in the tests were analysed using the SmartSEM GUI software programme.

Test Materials

Steels used in the laser welding tests are presented in Table 4.1. The technological laser welding tests involved the making of T-joints using flat bars (30 × 100 × 1 mm and 30 × 100 × 3 mm). The 3 mm thick flat bar constituted the shelf

(flange) of the T-joint and simulated the wall of a fin tube. The 1 mm flat bar was the web of the T-joint and simulated band iron wound on a tube (the fin of a fin tube). Appropriately-sized specimens were cut out of steel sheets using laser. The test materials were subjected to chemical composition analyses. The results of chemical composition analyses are presented in Table 1. It should be noted that various thicknesses of the same material grade were characterised by different contents of chemical elements (restrained within the range defined by related standards). Only steel 310 revealed the chromium content amounting to 23.39% (1 mm thick sheets) and 23.55 % (3 mm thick sheets) and was lower than the chromium content variability range of 24.0% to 26.0%, defined by PN-EN 10095:2002: Heat Resisting Steels and Nickel Alloys.

Table 1. Chemical compositions of the austenitic steels used in the tests

Chemical element	Content [% by weight]					
	304 (X5CrNi18-10, 1.4301)		304H (X6CrNi18-10, 1.4948)		310 (X15CrNiSi25-21, 1.4841)	
	1 mm	3 mm	1 mm	3 mm	1 mm	3 mm
C	0.024	0.022	0.049	0.050	0.054	0.053
Si	0.358	0.284	0.460	0.345	1.62	1.83
Mn	1.45	1.76	1.63	1.23	1.36	1.46
P	0.003	0.005	0.004	0.004	0.002	0.001
S	0.003	0.003	0.003	0.003	0.002	0.002
Cr	17.49	17.93	17.96	17.79	23.39	23.55
Mo	0.332	0.369	0.0360	0.209	0.167	0.141
Ni	9.98	9.20	9.16	9.03	19.97	20.07
Cu	0.418	0.511	0.433	0.235	0.260	0.199
Al	<0.001	0.002	0.003	0.007	0.010	0.037
Co	0.185	0.179	0.119	0.188	0.251	0.255
Nb	0.019	0.011	0.008	0.006	0.005	0.006
Sn	0.010	0.010	0.008	0.006	0.006	0.007

Tests and Analysis of Test Results

The initial parameters of the laser welding of the T-joints made of steel 304 (3 mm + 1 mm) were obtained when remelting the 1 mm thick sheet made of steel 304. For each type of laser (CO₂ and Yb:YAG) and three levels of laser beam power, welding rates (Table 2) were adjusted in a manner ensuring the obtainment of the full penetration of sheets for properly placed “scales” containing faces and roots. The welding parameters were used during the welding of the test T-joints and were accordingly modified in relation to base materials used in the tests. Because of a relatively low welding rate of 1.5 m/min, tests involving the use of the CO₂ laser and a power of 2200 w were not performed.

The tests revealed significant differences in welding rates obtained using the CO₂ and the Yb:YAG solid-state laser. The differences could be attributed to various laser radiation wavelengths, various power density in the focusing point (various laser beam focus diameters) and various power density distribution in the focus (Fig. 2 and 4). The shorter Yb:YAG laser radiation beam is better absorbed by materials

being welded; lower laser beam power ensures the obtainment of the same penetration depth. The differences could result from different laser designs and methods used when measuring laser beam power also used for adjusting energy pumping the active medium of the laser. In cases of disc lasers, measurements performed in the resonator are scaled in relation to measurements of laser beam power at the optical fibre output. Because of constant power losses in the optical fibre, calibration performed once is responsible for the fact that the adjustment of appropriate power level in laser settings corresponds to the actual power of laser beam striking the material, reduced by losses (if any) resulting from the condition of working head optics (e.g. impure protective glass). In cases of CO₂ lasers, power measured at the resonator output is also scaled in relation to the power of the laser beam striking the material, after passing through the system of mirrors transporting laser radiation to the working head. The status of mirrors is variable in time and may cause the reduction of the actual power of the laser beam striking the material.

Table 2. Selected output parameters for the melting of 1 mm thick sheets made of steel 304 in relation to different types of lasers used in the tests

TruLaserCell 1005 with the CO ₂ laser			TruLaser Robot 5120 with the TruDisk Yb:YAG laser		
Laser beam power [W]	Welding rate [m/min]	Welding linear energy [kJ/mm]	Laser beam power [W]	Welding rate [m/min]	Welding linear energy [kJ/mm]
2 200	1.5	0.0880	2 200	5	0.0264
3 000	3.5	0.0514	3 000	7	0.0257
3 800	4.0	0.0570	3 800	9	0.0253

Effect of the Laser Beam Position in Relation to the Joint Axis on the Process of Laser Welding

The obtainment of proper T-joints having butt welds with full penetration is influenced not only by welding linear energy parameters (laser beam power and welding rate), but also by the proper positioning of the T-joint–laser beam system (Fig. 5). The laser beam should melt the interface of elements being welded, which, when solidifying, form a weld. Because of the joint shape (T-like shape), the direction of laser beam propagation cannot be adjusted in accordance with the axis of the interface of elements being joined. The proper adjustment of the geometrical parameters of the system: angle of laser beam insertion in the interface area – α [°], the position of the laser beam focus in relation to the T-joint flange surface – a [mm] and the shift of the laser beam focus in relation to the interface of sheets being joined (laser beam defocusing degree) f [mm] are decisive for the obtainment of properly shaped welds.

The initial welding tests performed using the CO₂ laser revealed that the most favourable

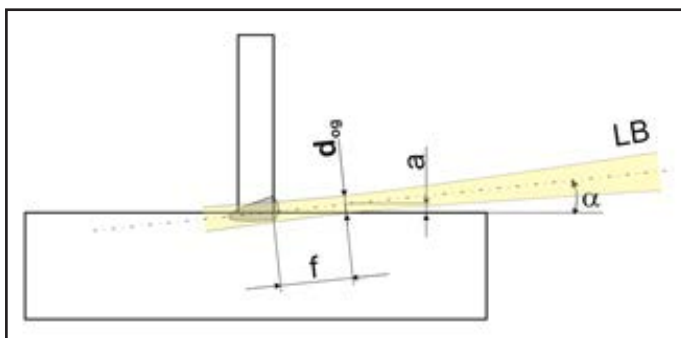


Fig. 5. Scheme of laser welded T-joint with the characteristic quantities of the laser beam position in relation to the interface of sheets being welded

positioning of the laser beam involved its focusing on the interface of elements being welded, without making any additional shifts (parameter $a = 0$ mm and $f = 0$ mm). Any changes, particularly those of parameter a disturbed welding and led to the obtainment of improper joints, or in extreme cases, to the complete lacks of joints. The position of a was determined optically, by observing the position of red coloured pilot laser radiation beam. To a significant extent, the accuracy of such positioning depends on the operator’s subjective impression, whereas the co-axiality of the laser beam (CO₂ laser) and of the red pilot laser beam (He-Ne laser) depend on the accuracy of pilot laser adjustment. Because of various wavelengths of CO₂ and pilot laser radiation, the optimum adjustment of the system proved difficult and the pilot laser beam focus was shifted in relation to the CO₂ laser focus along the optical axis of laser beam propagation.

The Yb:YAG solid-state laser proved to offer the significantly greater possibility of changing parameters a and f . In many welding tests, angle α remained unchanged, only the distance of laser beam focus f (Fig. 5) from the interface of sheets making up the T-joint (laser beam defocusing degree) and the position of the laser beam focus a (Fig. 5) in relation to the T-joint flange surface were modified. Welding tests were performed using a beam power of 2.2 kW and a reduced welding rate of 3 m/min. The welding rate was reduced in order to ensure the obtainment of an appropriate penetration depth. The reduced welding rate was also used in welding tests involving the defocusing the laser beam so that welding imperfections, if any, would only

result from the inappropriate positioning of the laser beam and not from overly low heat input to the joint. Exemplary macrostructures of the welded joints made of steel 304 are presented in Figure 6. The tests revealed that the range of laser beam defocusing degree enabling the obtainment of proper joints was relatively wide ranging from $f = 0$ mm to $f = 4$ mm. The laser beam defocusing amounting to $f = 4$ mm significantly reduced the penetration depth (Fig. 6 j l) and in cases of higher laser welding rates might result

in lacks of penetration. In addition, the increase in the laser beam defocusing degree above $f = 3$ mm deteriorated the aesthetics of the weld face, causing the formation of intermittent undercuts and incompletely filled grooves. The welding tests performed using modified positions of the laser beam in relation to the T-joint flange surface a revealed the significant importance of this parameter as regards the obtainment of proper welds. Failure to lift the laser beam in relation to the T-joint flange surface resulted in

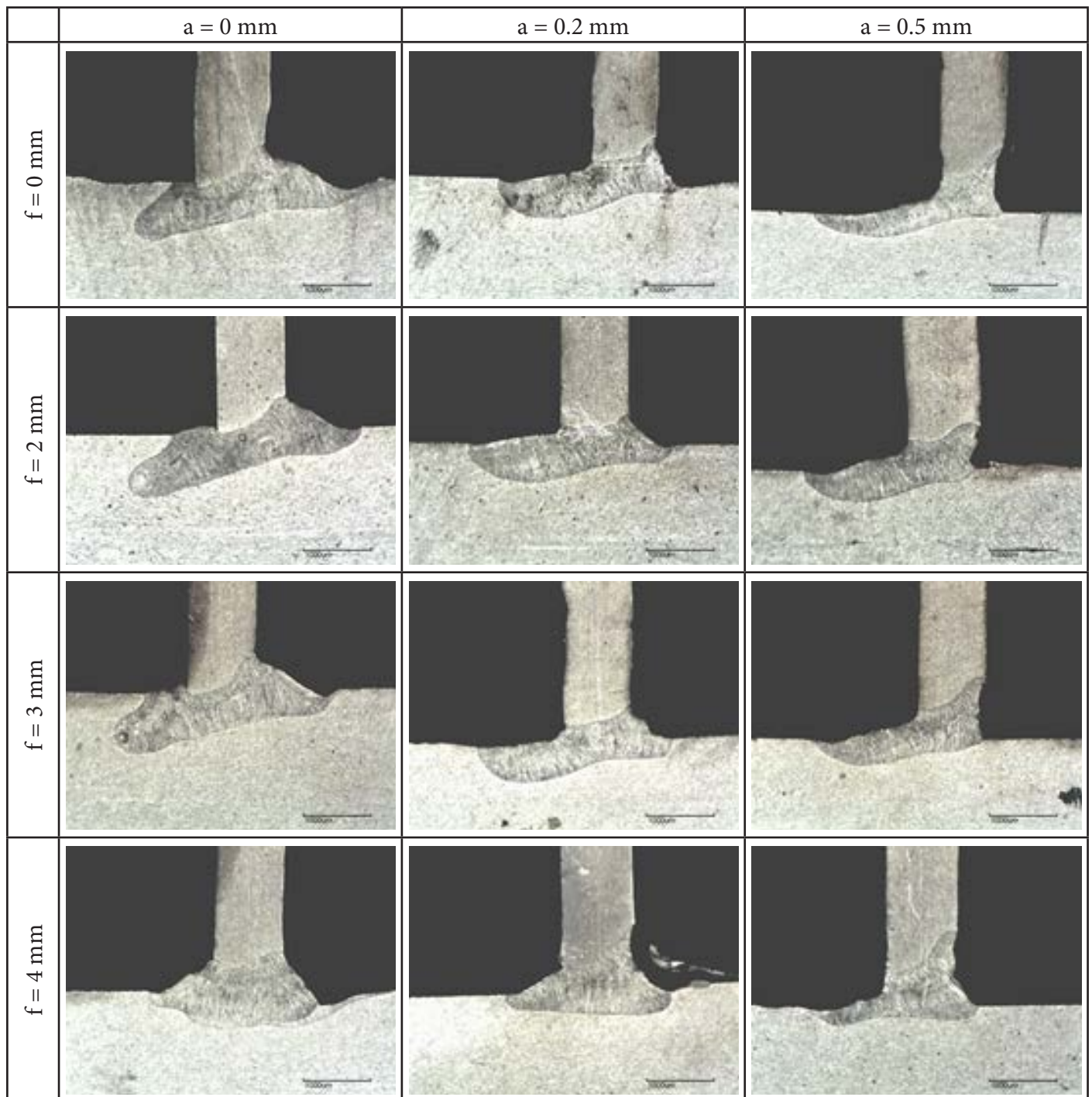


Fig. 6. Exemplary macrostructures of the T-joints made of steel 304 at various laser beam defocusing degrees f and various positions of the Yb:YAG laser beam in relation to the surface of the T-joint flange a

the increased probability of lacks of penetration in weld roots (Fig. 6 a). The above-named imperfection is nearly impossible to detect using visual tests; the entire image of the imperfection is only possible on metallographic specimens. The shape of the weld root run is asymmetric because of different heat discharge conditions in this area. The lack of intense heat discharge near the T-joint flange surface increased the volume of molten metal and led to the partial melting of the flange surface. The molten metal surrounded the unmelted joint interface area (Fig. 7). The increased laser beam defocusing degree slightly increased the width of the weld, not ensuring the obtainment of proper penetration. Only defocusing $f = 4$ mm led to the sharp decrease in penetration depth and the increase in the weld width (Fig. 4.14j). Changing the beam position within the range of $a = 0.2$ mm ÷ 0.5 mm enabled the obtainment of a proper weld root. The

further increase in distance a resulted in welding process instability. When $a = 1$ mm, the laser beam punctured the T-joint flange without melting the interface on the weld face side (Fig. 8). On the basis of related analysis, the parameters selected for further Yb:YAG laser welding tests were $a = 0.2$ mm and $f = 2$ mm.

CO₂ laser welding of T-Joints

Tests involving welding performed using the CO₂ laser were conducted for two different laser beam values adjusted on the control panel (Table 3). The laser beam was focused on the interface of elements being joined and was led at an angle of 160 in relation to the surface of the T-joint base. Exemplary macrostructures as well as weld faces and weld roots of properly made joints are presented in Figures 9÷12. The joints were characterised by very good quality revealed in visual and macroscopic tests. The weld roots of the joints were properly shaped. In some cases, the weld faces revealed slight undercuts only visible in macrographic photographs at large magnification.

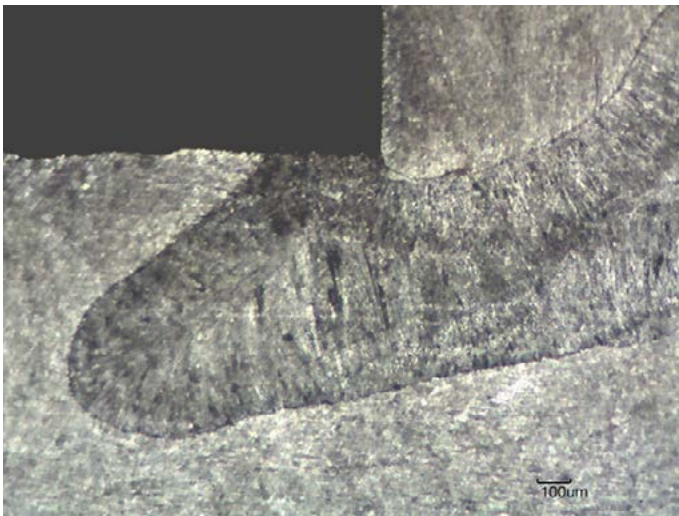


Fig. 7. Weld root of the T-joint made of steel 304 using $f = 0$ mm and $a = 0$ mm

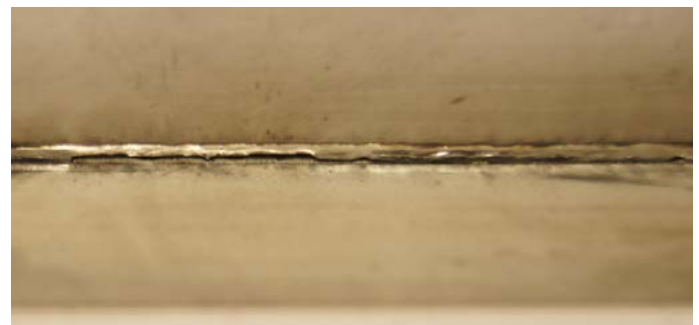


Fig. 8. Weld face of the T-joint made of steel 304 using parameters $a = 1$ mm and $f = 2$ mm

Table 3. Process parameters used during the CO₂ laser welding of 3 mm + 1 mm steel T-joints

Material	Number of set of parameters	Laser beam power [W]	Welding rate [m/min]	Linear energy [kJ/mm]	Position of laser beam focus	
					f [mm]	a [mm]
304 (X5CrNi18-10)	1	3000	3.5	0.0514	0	0
	2	3800	4.0	0.0570	0	0
304H (X6CrNi18-10)	3	3000	3.5	0.0511	0	0
	4	3800	4.0	0.0570	0	0
310 (X15CrNiSi25-21)	5	3000	3.5	0.0514	0	0
	6	3800	4.0	0.0570	0	0

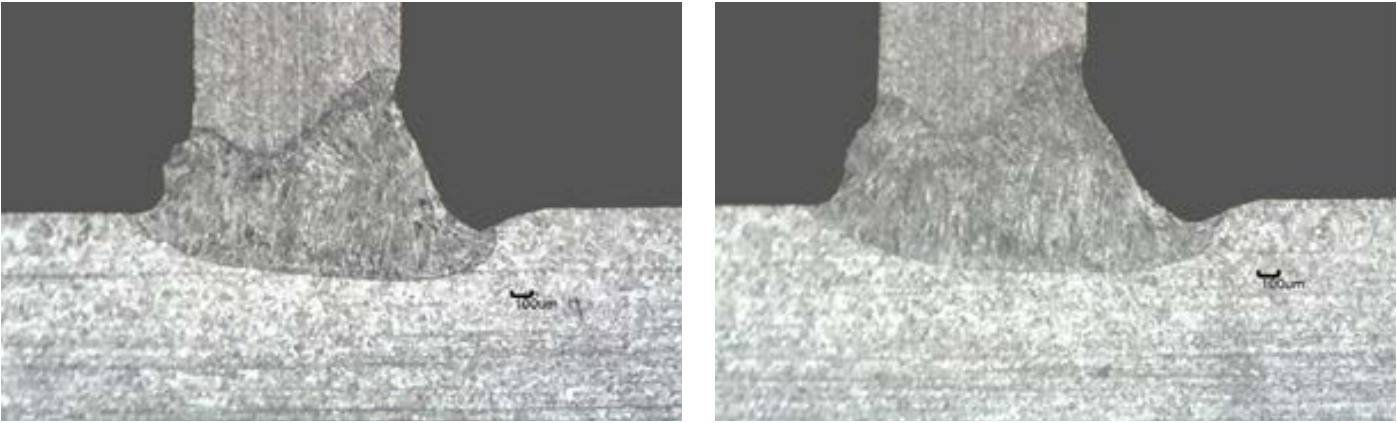


Fig. 9. Macrostructure of the CO₂ laser welded T-joint made of steel 304 a) parameters no. 1, b) parameters no. 2 (Table 3)

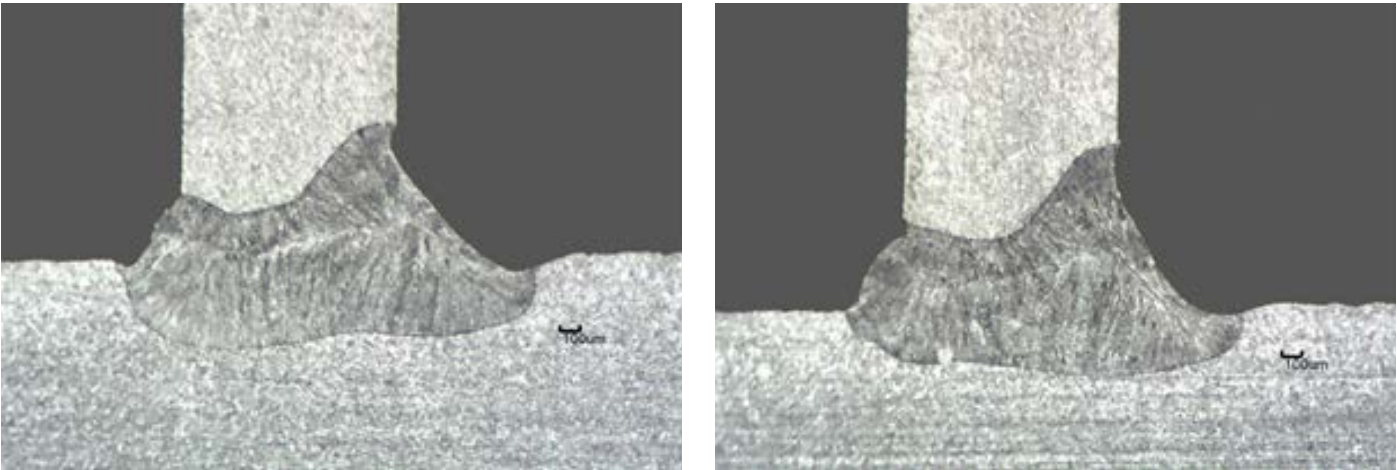


Fig. 10. Macrostructure of the CO₂ laser welded T-joint made of steel 304H a) parameters no. 3, b) parameters no. 4 (Table 3)

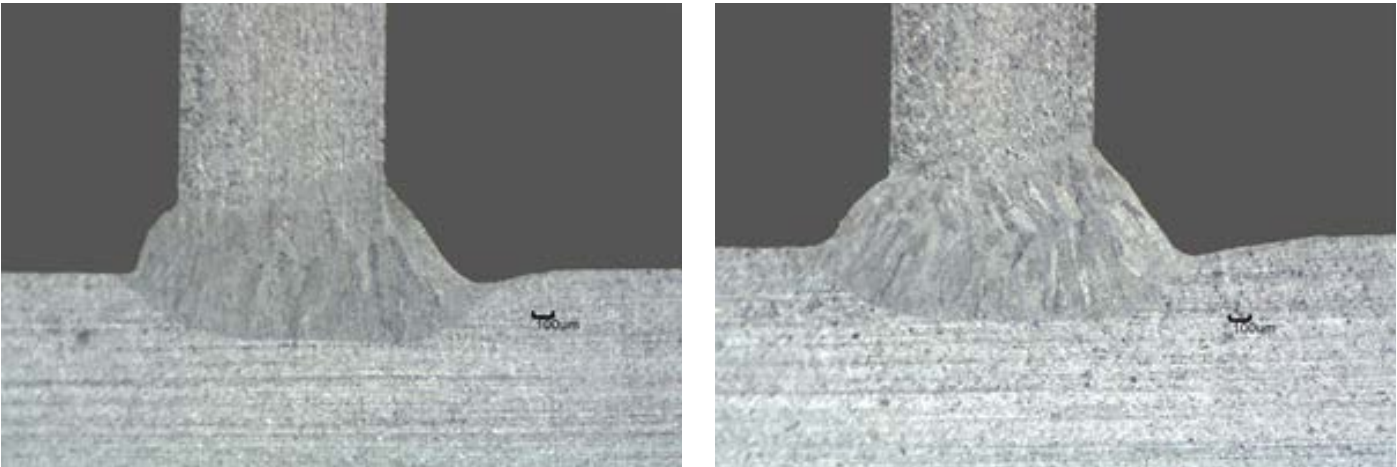


Fig. 11. Macrostructure of the CO₂ laser welded T-joint made of steel 310 a) parameters no. 5, b) parameters no. 6 (Table 3)

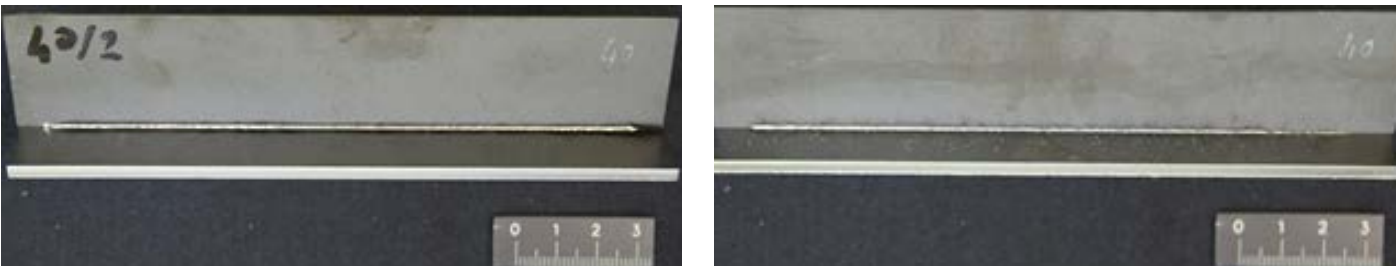


Fig. 12. Exemplary view of the face and root of the weld of the CO₂ laser welded T-joint made of steel 310, parameters no. 5, Table 3

The joints welded using the CO₂ laser beam having a power of 3800 W were tested using an electron microscope provided with an EDS spectrometer. The purpose of the microscopic test was to record any possible changes in contents of alloying components caused by the burning or the evaporation of alloying components during laser welding. The excessive depletion of alloying components in the weld could change the properties of steel in the weld area, which could significantly compromise the desired properties of structure in operation. The analysis of the chemical composition involved micro-areas located in three zones: the base material of T-joint shelf – zone no. 1, weld area – zone no. 2 and the base material of the web

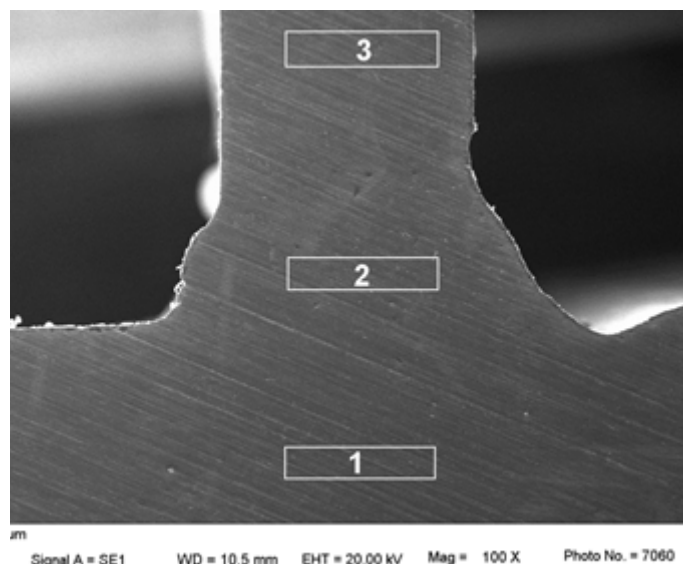
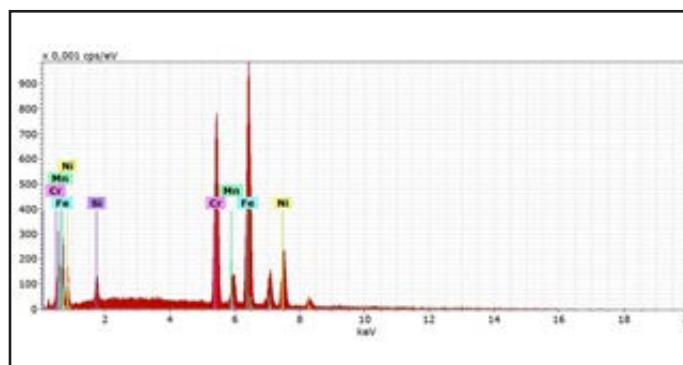
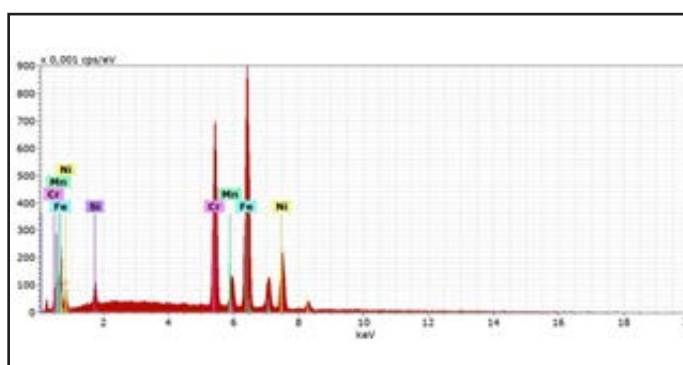


Fig. 13. Marked areas on the cross-section of the CO₂ laser welded T-joint subjected to the analysis of the chemical composition involving the use of electron microscope with the EDS spectrometer

Zone no. 1 (base material, t = 3 mm)		
Chemical element	[wt.%]	[at.%]
Fe	52.88	51.69
Mg	2.47	2.46
Cr	24.86	26.10
Ni	18.45	17.16
Si	1.34	2.60
Total	100.00	100.00



Zone no. 2 (weld)		
Chemical element	[wt.%]	[at.%]
Fe	53.39	52.36
Mg	2.55	2.54
Cr	24.12	25.41
Ni	18.87	17.60
Si	1.07	2.09
Total	100.00	100.00



Zone no. 3 (base material t = 1 mm)		
Chemical element	[wt.%]	[at.%]
Fe	53.59	52.53
Mg	2.75	2.74
Cr	23.79	25.04
Ni	18.72	17.45
Si	1.15	2.24
Total	100.00	100.00

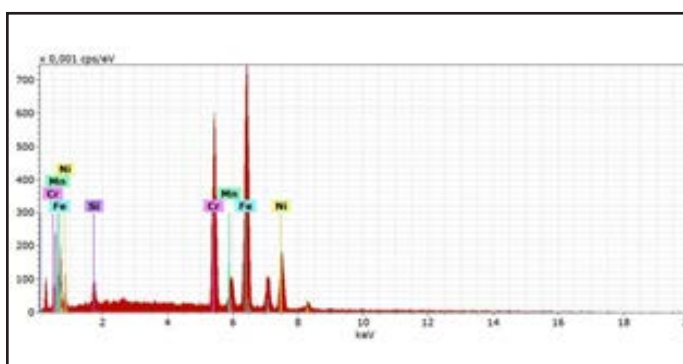


Fig. 14. Exemplary result concerning the chemical composition analysed in the individual zones of the CO₂ laser welded T-joint made of steel 310 (parameters no. 6, Table 3)

– zone no. 3 (Fig. 13-14). In addition, the tests involved the analysis of the distribution of alloying components on the cross-section of the joint (Fig. 15). The tests revealed that the process of laser welding did not trigger any significant changes in percentage contents of alloying components (Mn, Cr, Ni, Si) in the individual test zones of the T-joint. The percentage contents of individual alloying components in the weld was restricted between the values of percentage contents of individual alloying components in the base material of the flange and web of the T-joint. Only steel 310 revealed a slight decrease in the content of silicon (increasing the melting point and recrystallization point of the steel (Fig. 14).

Yb:YAG laser welding of T-Joints

Tests involving welding performed using the Yb:YAG laser were conducted for three different laser beam values adjusted on the control panel (Table 4). The laser beam was positioned at

an angle of 16° in relation to the surface of the T-joint base; the parameters of the laser beam focus position in relation to the interface between the test sheets were $f = 2 \text{ mm}$ and $a = 0.2 \text{ mm}$. Exemplary macrostructures as well as weld faces and (easily visible) weld roots of properly made joints are presented in Figures 16÷19. The T-joints made of steel 310 welded using the laser beam having a power of 2.2 kW and 3 kW (parameters no. 13 and 14, Table 4) revealed single local weld root area reductions indicating process instabilities or difficulties connected with the formation of roots in steel 310. The joints welded using a power of 3.8 kW, made of all steel grades (parameters no. 9, 12 and 15, Table 6), were characterised by properly shaped weld roots, often wider than weld faces (containing slight porosity-like irregularities). If subjected to operation in aggressive environments, such irregularities could favour the deposition of sediments precipitated from the environment surrounding the structure.

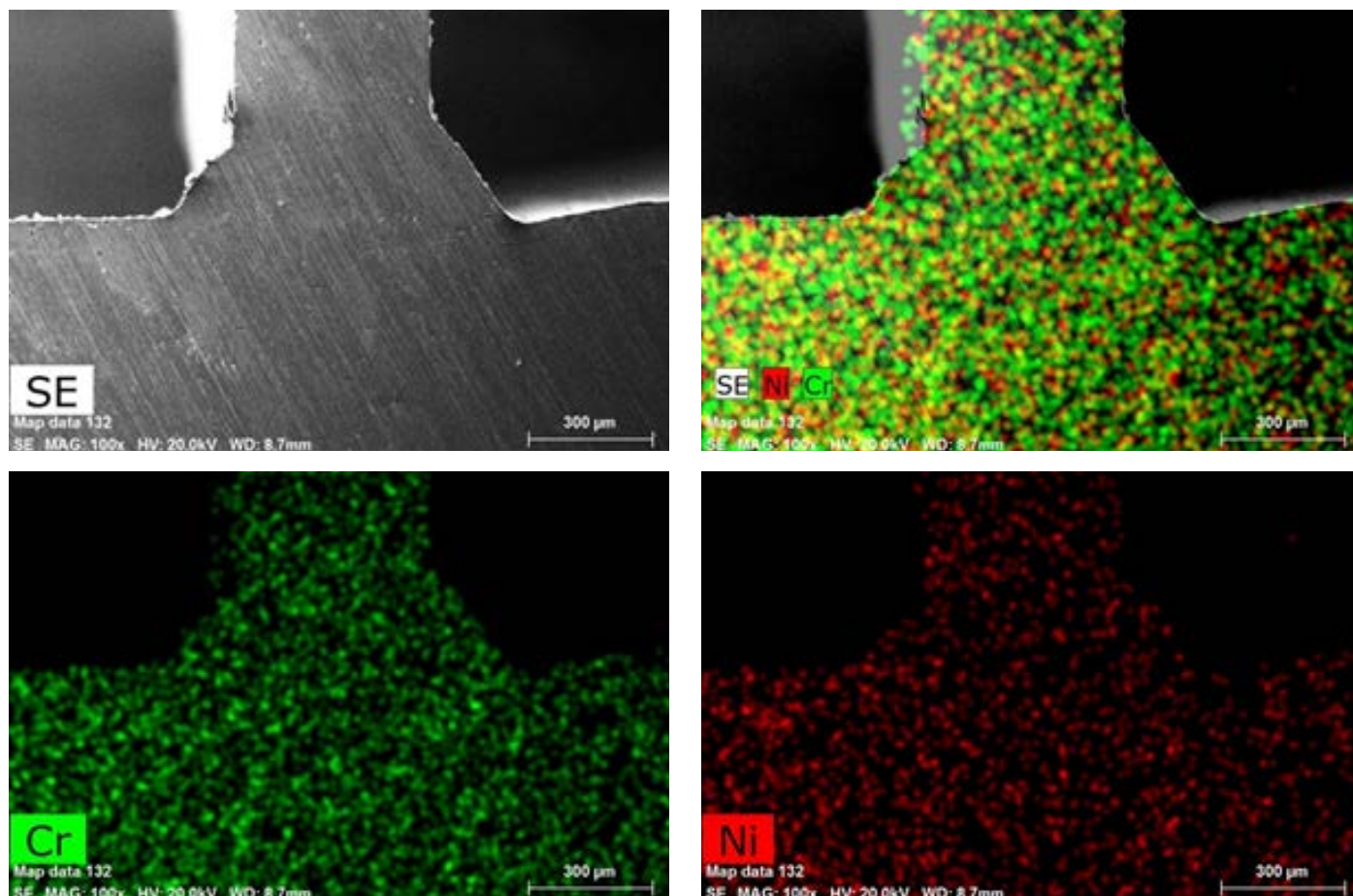


Fig. 15. Exemplary distribution of chromium (Cr) and nickel (Ni) on the cross-section of the CO₂ laser welded T-joint made of steel 310 (parameters no. 6, Table 3)

Table 4. Process parameters used during the Yb:YAG laser welding of 3 mm + 1 mm steel T-joints

Material	Number of set of parameters	Laser beam power [W]	Welding rate [m/min]	Linear energy [kJ/mm]	Position of laser beam focus	
					f [mm]	a [mm]
304 (X5CrNi18-10)	7	2200	9	0.0147	2	0.2
	8	3000	11	0.0164	2	0.2
	9	3800	11	0.0207	2	0.2
304H (X6CrNi18-10)	10	2200	9	0.0147	2	0.2
	11	3000	11	0.0164	2	0.2
	12	3800	11	0.0207	2	0.2
310 (X15CrNiSi25-21)	13	2200	9	0.0147	2	0.2
	14	3000	11	0.0164	2	0.2
	15	3800	11	0.0207	2	0.2

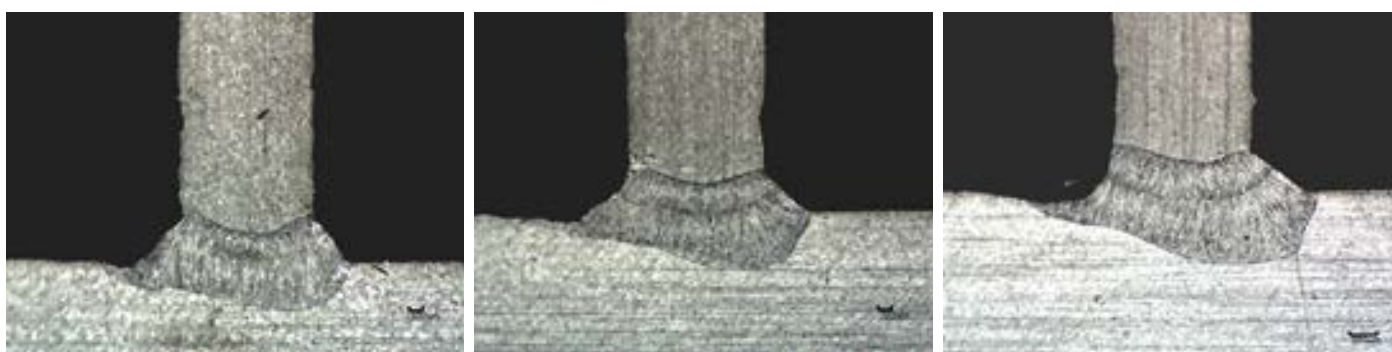


Fig. 16. Macrostructure of the Yb:YAG laser welded T-joint made of steel 304 a) parameters no. 7, b) parameters no. 8, c) parameters no. 9 (Table 4)

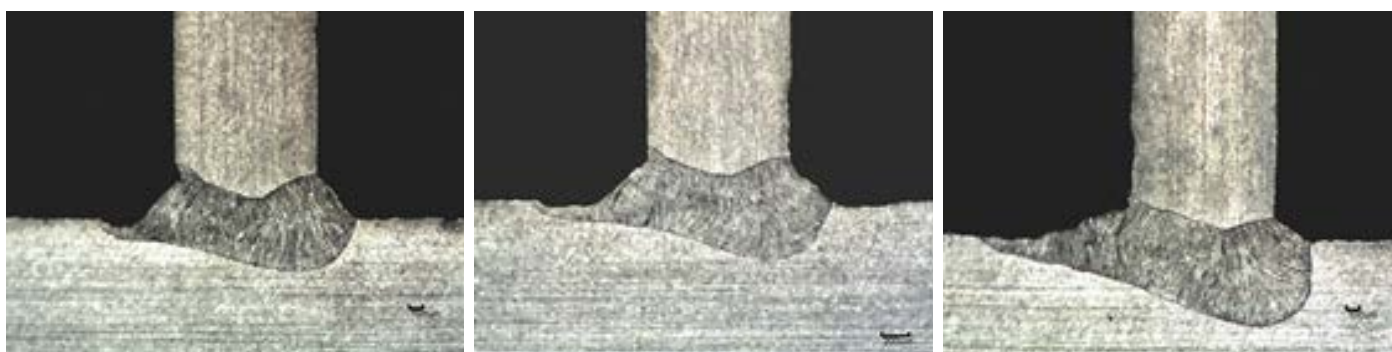


Fig. 17. Macrostructure of the Yb:YAG laser welded T-joint made of steel 304H a) parameters no. 10, b) parameters no. 11, c) parameters no. 12 (Table 4)

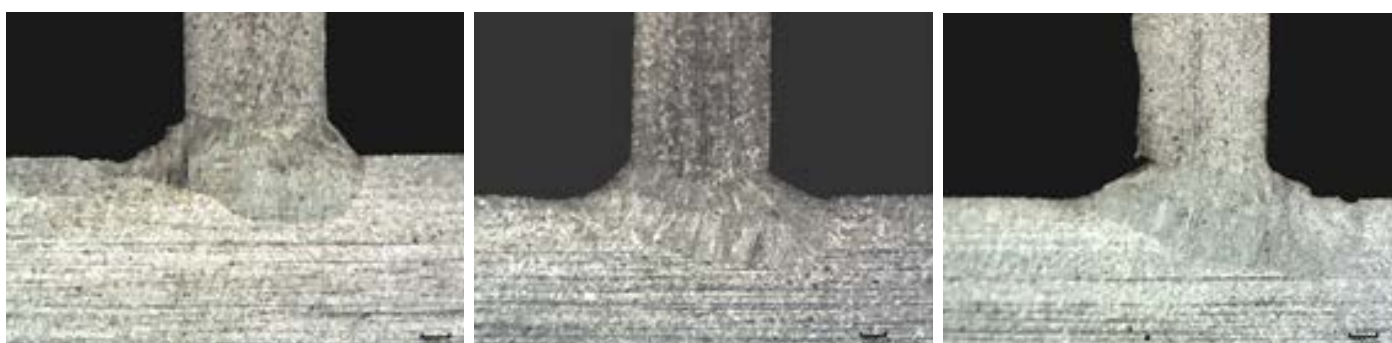


Fig. 18. Macrostructure of the Yb:YAG laser welded T-joint made of steel 310 a) parameters no. 13, b) parameters no. 14, c) parameters no. 15 (Table 4)

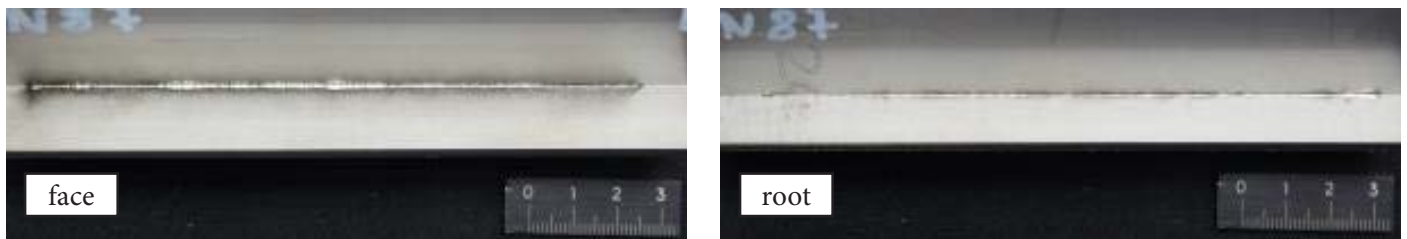
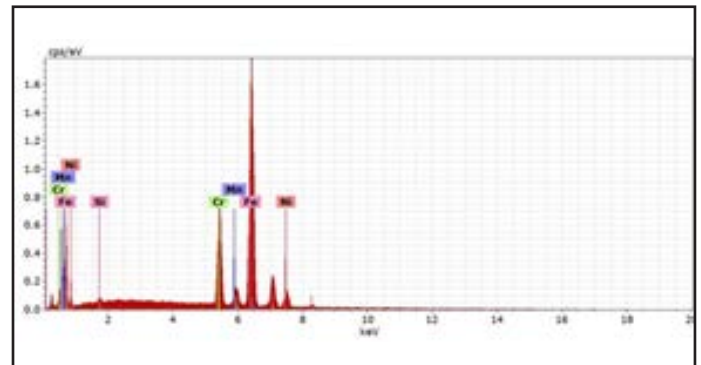


Fig. 19. Exemplary view of the face and root of the weld of the Yb:YAG laser welded T-joint made of steel 304H, parameters no. 11, Table 4

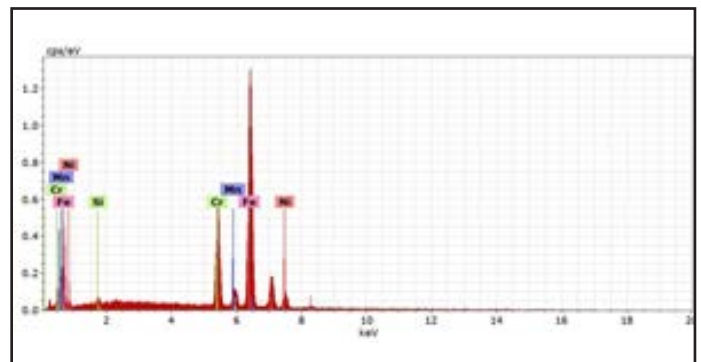
Similar to the tests of the joints made using the CO₂ laser, the joints welded using the Yb:YAG laser beam having a power of 3800 W were tested using an electron microscope provided with an EDS spectrometer. The purpose of the microscopic test was to record any possible changes in contents of alloying components caused by the burning or the evaporation of alloying components during laser welding.

The analysis of the chemical composition involved micro-areas located in three zones: the base material of T-joint shelf – zone no. 1, weld area – zone no. 2 and the base material of the web – zone no. 3 (Fig. 13, 20). In addition, the tests involved the analysis of the distribution of alloying components on the cross-section of the joint (Fig. 21). The tests revealed that the process of laser welding did not trigger any

Zone no. 1 (base material, t = 3 mm)		
Chemical element	[wt.%]	[at.%]
Fe	71.76	70.91
Mn	3.17	3.18
Cr	17.19	18.24
Ni	7.63	7.17
Si	0.25	0.49
Total	100.00	100.00



Zone no. 2 (weld)		
Chemical element	[wt.%]	[at.%]
Fe	71.63	70.66
Mn	3.29	3.29
Cr	17.10	18.12
Ni	7.56	7.09
Si	0.42	0.83
Total	100.00	100.00



Zone no. 3 (base material ≠1 mm)		
Chemical element	[wt.%]	[at.%]
Fe	70.71	69.76
Mn	3.39	3.40
Cr	17.81	18.87
Ni	7.71	7.23
Si	0.37	0.73
Total	100.00	100.00

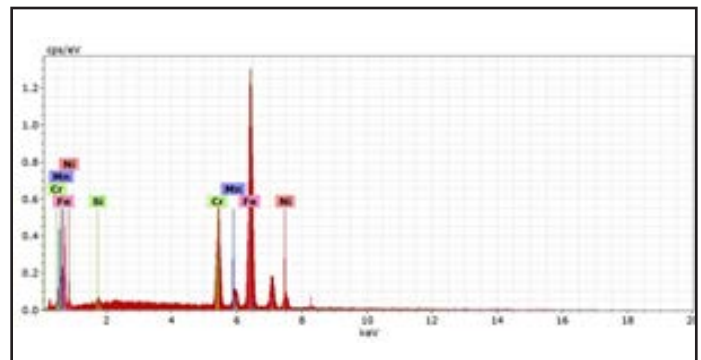


Fig. 20. Chemical composition analysed in the individual zones of the Yb:YAG laser welded T-joint made of steel 304H (parameters no. 12, Table 4)

significant changes in percentage contents of alloying components (Mn, Cr, Ni, Si) in the individual test zones of the T-joint. The joints made of steel 304H and 310 revealed a slight decrease in nickel content.

Summary

The tests revealed that it was possible to make proper T-joints with butt welds made of laser beam welded alloy steels. The making of the above named joints was possible using both gas (CO₂) and solid state (Yb:YAG) lasers.

It was ascertained that during the laser welding of T-joints with butt welds, the obtainment of full penetration was influenced by the position of the interface (i.e. edges) of elements being joined and the position of the laser beam. Because of the focused laser beam shape in the space (laser beam caustic curve) and due to the

type of a joint, the direction of laser beam propagation could not be set in accordance with the axis of the interface of elements being joined. For this reason, it was necessary to adjust an appropriate laser beam inclination angle in relation to the surface of the T-joint flange. The minimum laser beam inclination angle $\alpha = 16^\circ$ adjusted in the tests enabled the obtainment of properly shaped welds. In addition, the slight defocusing of the Yb:YAG laser beam, i.e. $f = 2 \text{ mm}$ enabled the obtainment of an aesthetic weld face, whereas lifting the laser beam by $a = 0.2 \text{ mm}$ resulted in the full penetration of the weld root.

Changing the type of laser used for the welding of T-joints required changes in primary process parameters, i.e. laser beam power values and welding rates. The tests revealed that the use of a solid-state laser having the same

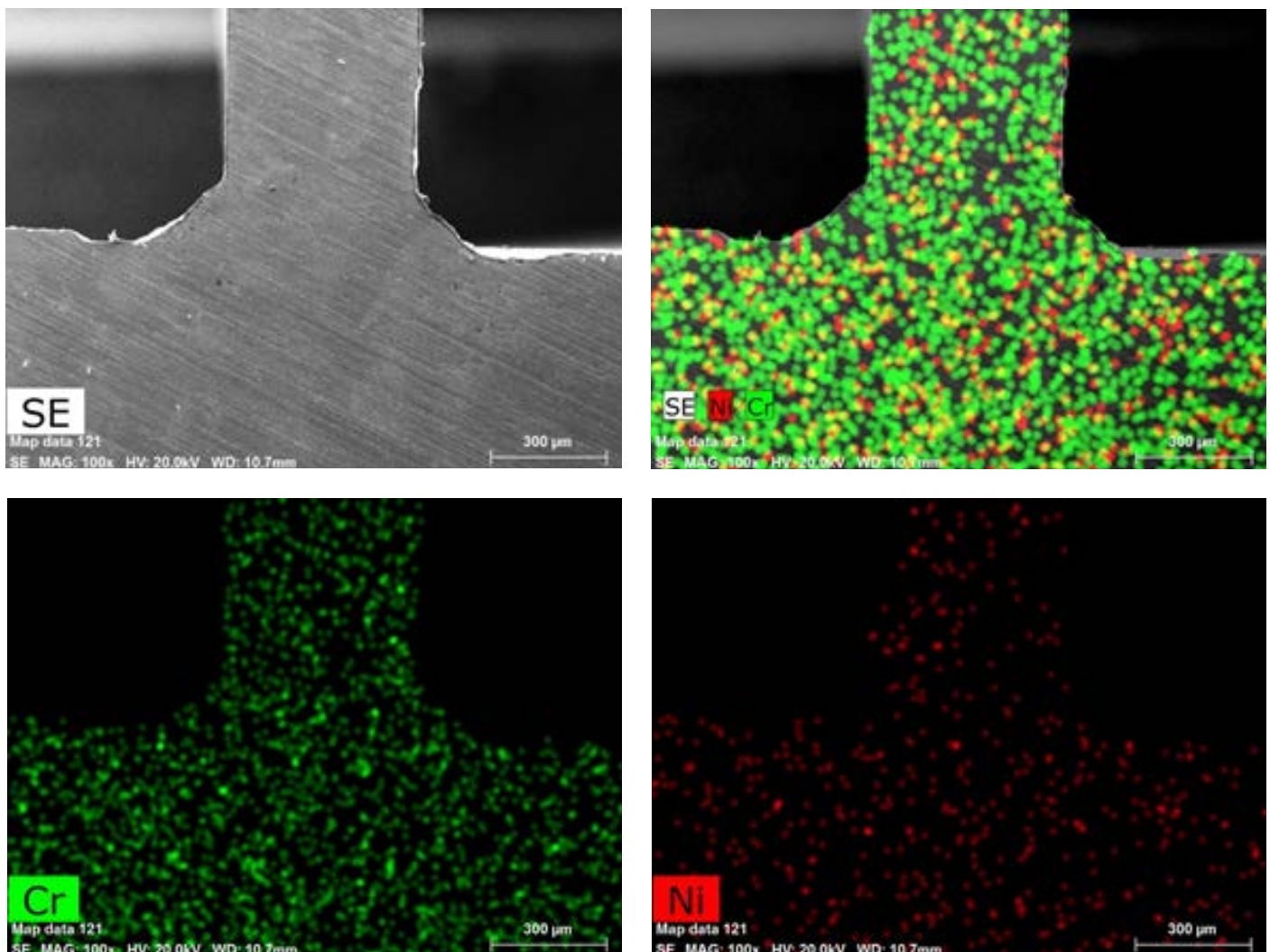


Fig. 21. Distribution of chromium (Cr) and nickel (Ni) on the cross-section of the Yb:YAG laser welded T-joint made of steel 304H (parameters no. 12, Table 4)

laser beam power adjusted on the operator control panel increased the welding rate multiple times. The rate obtained when welding steel joints using a beam power of 3 000 w was nearly three times higher when the Yb:YAG laser was used than the welding rate obtained using the same beam power and the CO₂ laser (Tables 3 and 4, Fig. 22). Such a significant increase in the welding rate was primarily caused by the difference in the absorption of laser

radiation having a given wavelength. A nearly ten times shorter electromagnetic wave generated by Yb:YAG lasers was better absorbed by metallic materials.

The laser welding of 3 mm and 1 mm thick T-joints was not accompanied by significant percentage changes in contents of alloying components in the weld and in the base material.

The research was financed using funds of project PBS1/A5/13/2012.

References

[1] Breeze P.: *Raising steam plant efficiency – Pushing the steam cycle boundaries*. PEI Magazine, 2012 April, Vol. 20, Issue 4.

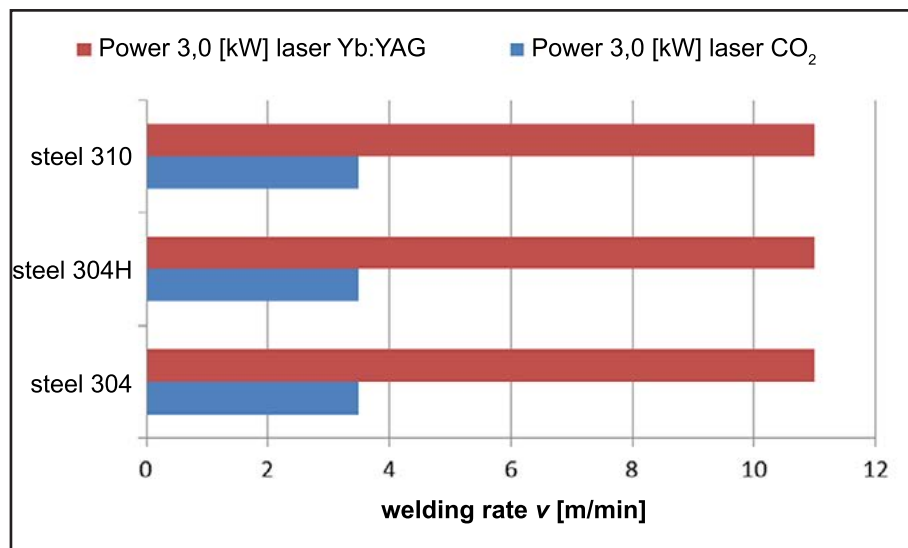


Fig. 22. Comparison of laser welding rates in relation to individual steel grades and types of lasers

[2] Huseman R.: *Advanced (700°C) PF Power Plant. A Clean Coal European Technology*. Advanced Material for AD700Boilers, Cesi Auditorium, Milano, 2005.

[3] Najgebauer E., Patrycy A.: *Zobowiązania polskiej energetyki wobec EU* <http://geoland.pl/>

[4] Hernas A., Pasternak J., Brózda J., Moskal G.: *Stale austenityczne i nadstopy niklu stosowane do budowy kotłów nadkrytycznych i ultranadkrytycznych*. Wyd. SITPH, Katowice 2009

[5] Adamiec J., Gawrysiuk W., Więcek M.: *Zautomatyzowane stanowisko do spawania rur ożebrowanych laserem*. Biuletyn Instytutu Spawalnictwa, 2010, no. 5.